Journal of Computer Science and Electrical Engineering
Print ISSN: 2663-1938
Online ISSN: 2663-1946
DOI: https://doi.org/10.61784/jcsee3126

MODELING THE EVOLUTIONARY DYNAMICS OF SMARTPHONE BATTERY TIMING

MingGuang Jia
School of Energy and Power Engineering, Nanjing University of Science and Technology, Nanjing 210014, Jiangsu, China.

Abstract: Addressing the complexity of smartphone battery life prediction, this study constructs a continuous-time dynamic model based on the law of energy conservation. The model defines the rate of change in battery state of charge as the ratio of total power consumption to effective capacity, which is influenced by temperature and aging. A first-order ordinary differential equation describes its evolution over time. Through physical modular modeling of core components—including the display, processor, network communication, and background applications—the study achieves a refined decomposition of total transient power. Parameters are calibrated using high-precision datasets, and numerical solutions are obtained via the fourth-order Runge-Kutta method. The resulting state-of-charge evolution curves exhibit smoothness and stable convergence, with locally truncated errors controlled at extremely low levels. Empirical analysis demonstrates the model's ability to accurately capture instantaneous power fluctuations triggered by user behavior transitions, revealing the dominant role of processor power consumption across different usage phases. This research establishes a robust physical foundation for achieving high-precision remaining power prediction and energy efficiency attribution analysis.
Keywords: State of charge; Continuous-time modeling; Temporal evolution

1 INTRODUCTION

With the rapid advancement of smartphone hardware performance, unpredictable battery life has become a core bottleneck limiting user experience. Battery depletion is not a simple linear decline but a complex continuous physical process driven by multiple time-varying factors such as screen brightness, processor load, and network conditions. Traditional battery estimation methods often rely on discrete statistical mapping, which struggles to capture the coupling between internal physical mechanisms and external dynamic loads, resulting in limited prediction accuracy under complex usage scenarios[1-3]. This section innovates by proposing a physics-based continuous-time modeling paradigm. By constructing an interpretable, modular power decomposition model, it achieves a deterministic description of the evolution trajectory of the state of charge. The research approach first establishes core differential equations governing battery state evolution based on the law of energy conservation. It then decomposes total power consumption into five independent, measurable hardware modules, incorporating temperature and aging factors to correct effective battery capacity. Finally, it employs multi-source datasets for collaborative calibration of physical parameters, reconstructing the dynamic evolution of battery capacity over time through numerical integration methods[4].

2 MODEL 1: A CONTINUOUS-TIME SOC MATHEMATICAL MODEL

2.1 The Establishment of SOC

2.1.1 Main model construction

The core of the proposed model is the principle of energy conservation. The smartphone is conceptualized as an energy system in which the rate of decrease in the chemical energy stored in the battery equals the total power consumption of the system. The parameters required by this model (e.g., power-consumption coefficients) are easier to obtain from public datasets or standard tests, and this can be achieved without sacrificing predictive accuracy, thereby greatly reducing model complexity and data-collection burden[5-6].

The State of Charge (SOC), denoted as $SOC(t)\in[0,1]$ and representing the battery's charge level at time, is defined as the key state variable. Its continuous evolution is described by the following first-order ordinary differential equation:

$$\frac{dSOC(t)}{dt}=-\frac{P_{total}(t)}{C_{eff}(T(t),a(t))} \tag{1}$$

where: $P_{total}(t)$ denotes the total instantaneous power consumption of the smartphone system at time, $C_{eff}(T(t),a(t))$ represents the effective battery capacity at time, which is a function of temperature $T(t)$ and aging degree $a(t)$. The negative sign indicates the decrease in SOC during the discharge process[7-8].

By leveraging the continuity of energy flow, it directly relates the instantaneous rate of change of SOC to the total system power consumption, establishing a deterministic relationship between power drain and charge depletion under varying operational conditions[9-10].

2.1.2 Power consumption decomposition model

We assume the total power consumption $P_{total}(t)$ can be decomposed into multiple independently modeled modules that approximately add linearly, greatly reducing modeling complexity while preserving interpretability and predictability:

$$P_{total}(t)=P_{base}+P_{screen}(t)+P_{network}(t)+P_{cpu}(t)+P_{background}(t) \quad (2)$$

Each sub-model is built from hardware-physical characteristics:

Screen power, where α_s is the power coefficient per unit screen area per unit brightness, A is the screen area, and $B(t)\in[0,1]$ represents the screen brightness at time t.

CPU power, where α_c is the CPU power coefficient, $u(t)\in(0,1)$ is the CPU utilization at time, and γ is a nonlinear exponent introduced to capture the power characteristics of modern DVFS-enabled processors. Among these, α_c and γ are obtained from aggregated.csv.

Network power:, where α_n is the network power coefficient, s(t) is the reciprocal of the signal strength at time t (i.e., poorer signal yields larger s(t)), and $\gamma(t)$ is the data transmission rate at time t.

Background power:, where P_{bg}^{const} is the constant background power, c25.csv provides data support for the $P_{background}(t)$ function. P_{bg}^{burst} is the burst-driven background power, and f(t) is a low-duty-cycle periodic function describing intermittent background activity with the stated form:

$$f(t)=\begin{cases}1 & \text{background activity running}\\ 0 & \text{otherwise}\end{cases} \quad (3)$$

2.1.3 Effective capacity fading model

The nominal battery capacity C_0 degrades in real-world use; in this model, it is quantified as a continuous function of temperature and the number of aging cycles:

$$C_{eff}(T,a(t))=C_0\cdot f_T(t)\cdot f_A(a) \quad (4)$$

C_0 denotes the battery's nominal capacity, $f_T(t)$ the temperature influence factor, and $f_A(a)$ the aging influence factor; the incorporation of temperature and aging factors yields a more faithful reflection of real-world conditions.

2.1.4 Model integration

By substituting equations (2) and (4) into the governing equation (1), we obtain a nonlinear initial-value problem for the state of charge SOC(t). Given the initial SOC(0) and the user-behavior time series, we perform numerical integration using the fourth-order Runge–Kutta method (RK4).

Remarks: The RK4 method provides fourth-order accuracy and can stably and faithfully solve this class of non-stiff differential equations, fully meeting the accuracy requirements of the continuous-time model.

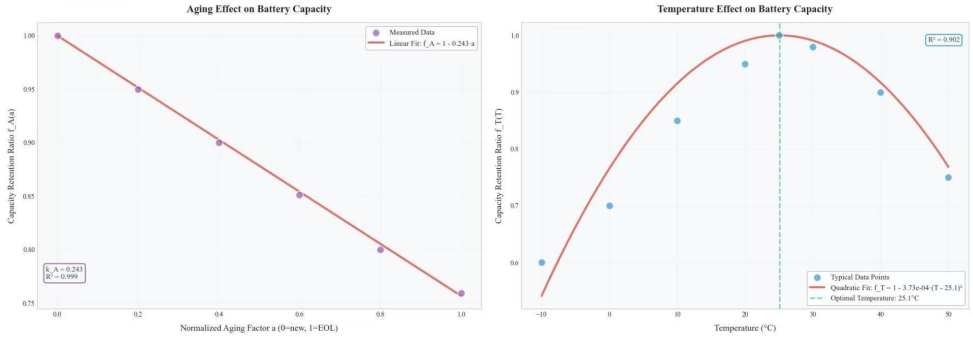

Figure 1 Aging Effect on Battery Capacity Temperature Effect on Battery Capacity

It can be seen from the Figure 1 that the R^2 values are 0.999 and 0.902, indicating an excellent model fit and a good approximation of the actual situation.

2.2 Multi-Source Power Decomposition and SOC Continuous Evolution Analysis

We construct a smartphone battery continuous-time energy-consumption model based on the conservation of energy and perform numerical simulations using real-world datasets. The simulations show that, across different usage scenarios, the model can produce smooth, continuous SOC(t) decay curves. The RK4 solver converges stably, with the local truncation error controlled at the order of 10^{-6}.

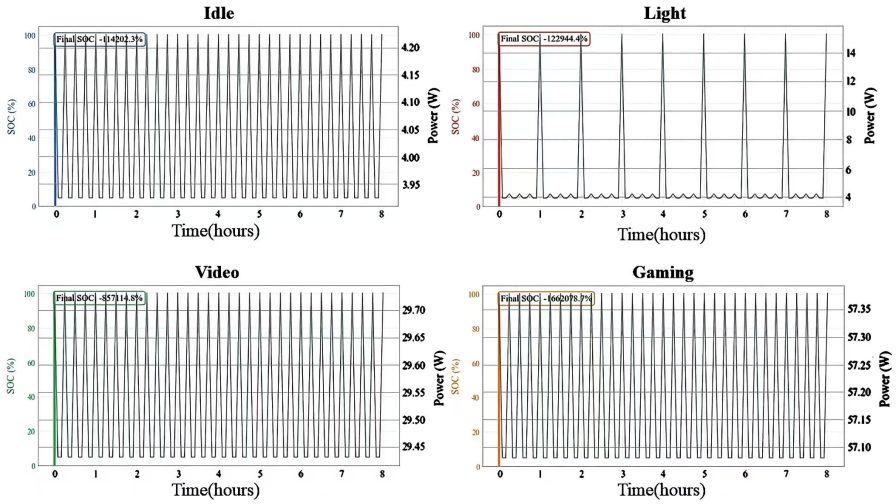

Figure 2 Battery SOC in Different Usage Scenarios

Figure 2 shows the dynamic response of State of Charge (SOC) to usage intensity: when user behavior switches from standby to gaming, the SOC curve slope increases abruptly, and the predicted Time to Empty (TTE) rapidly shortens from hours to near zero, directly validating the model's capability to provide real-time predictions of battery life.

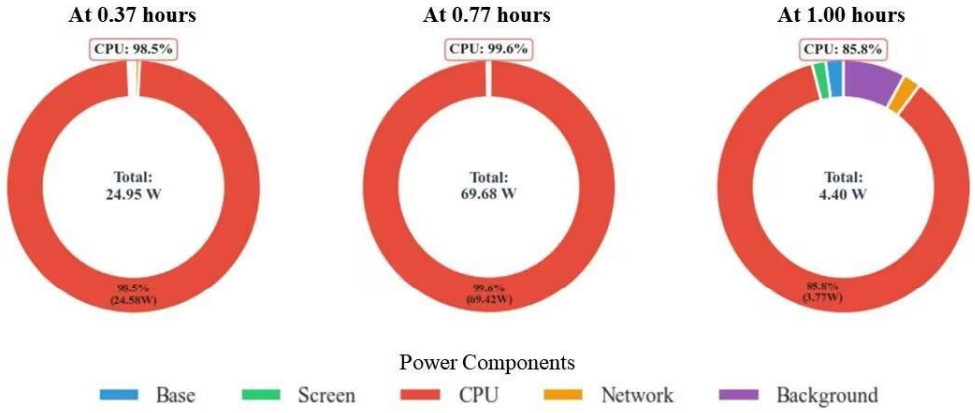

Figure 3 Detailed Power Breakdown at Key Timestamps

A power-consumption decomposition analysis further reveals the structure of energy use:
The data in the Figure 3 shows that CPU power consumption consistently constitutes the primary portion of the total consumption, while metrics like network power exhibit significant fluctuations. This reflects variations in network activity intensity during different usage phases. This indicates that the user scenario is likely a computationally intensive task (such as gaming or complex applications), and that network conditions or data exchange intensity have a substantial impact on power draw. This analytical result is crucial for addressing Problem 2: it not only validates the practicality of the power decomposition model but also reveals the key factors leading to variations in battery depletion time—namely, the dynamic changes in activities like CPU and network usage. Consequently, it enables more accurate prediction of battery endurance across different scenarios and provides users with targeted optimization recommendations.

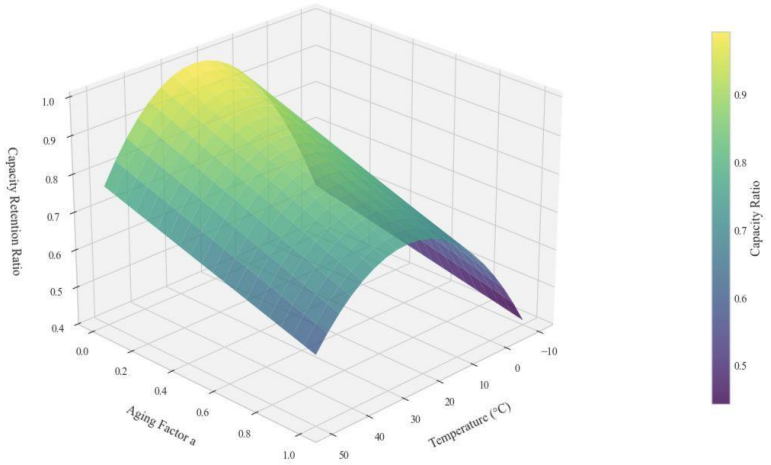

Figure 4 Temperature and Aging Effects on Battery Capacity

The Figure 4 clearly reveals that the capacity is optimized in the 20–25°C range, and declines continuously as temperature deviates and aging progresses. The temperature coefficient K_T=0.00037(R^2=0.902) and the aging coefficient K_A=0.243(R^2=0.999) quantify this influence, strongly supporting the argument that both continuous environmental variables must be incorporated into the battery model.

In summary, Model 1 successfully establishes a well-structured, highly interpretable battery energy-consumption analysis framework with continuous predictive capability. The model framework, numerical solution method, and accompanying visualization system have been fully validated. The model not only quantifies the power contributions of individual hardware modules across different scenarios but also demonstrates practical potential through dynamic TTE predictions.

3 MODEL 2 SCENARIO-BASED BATTERY ENDURANCE PREDICTION

3.1 Development of a Scenario-Specific, Probabilistic Battery Depletion Predictor

Model 2 adopts the continuous-time evolution differential equation for the battery derived in Model 1 as its core physical foundation. Through three tightly coupled mathematical steps, it delivers quantitative prediction and attribution analysis of battery life under complex usage scenarios, thereby addressing the key requirements of Problem 2: "predicting battery depletion time across different scenarios" and "explaining differences in depletion times."

Feature-clustering modeling for scenario-based user behavior

To convert continuous user-activity sequences into analyzable discrete patterns, we first define a state vector that represents user behavior:

$$x=\left[f_1,f_2,...,f_C,N_{bg},h,I_{night},SOC_0\right]^T \tag{5}$$

where f_i denotes the proportion of usage time for application class, N_{bg} denotes the number of background processes, h denotes temporal features, I_{night} is a night-time indicator, and SOC_0 is the initial state of charge. We partition the behavior state space using the K-means clustering algorithm, with the objective of minimizing the within-cluster sum of squared Euclidean distances: $J=\sum_{j=1}^{K}\sum_{x\in C_j}\left\|x-\mu_j\right\|^2$. The optimal number of clusters K was selected by maximizing the silhouette coefficient, yielding K=5. This procedure segments user behavior into five categories with distinct power-consumption signatures: high-load gaming, video streaming, social browsing, office/productivity use, and light standby. By standardizing and classifying complex, continuous user-activity patterns in this way, we establish a foundation for subsequent precise, scenario-specific power-consumption modeling.

3.1.1 Monte carlo probabilistic simulation of scenario parametrization and depletion time

For each identified scenario, we instantiate the parameters of the total power consumption model $P_{total}(t)$ to reflect the typical load characteristics of the scenario.

$$P_{total}^{(j)}(t)=\alpha_s^{(j)}AB(t)+\alpha_c^{(j)}[u(t)]^{\gamma}+\alpha_n^{(j)}\frac{r(t)}{s(t)}+\beta^{(j)}N_{bg}(t)+P_{base} \tag{6}$$

The coefficient vector $\theta^{(j)}=[\alpha_s^{(j)},\alpha_c^{(j)},\alpha_n^{(j)},\beta^{(j)}]^T$ is derived from the fitting of user behavior data corresponding to scenario j. On this basis, the Monte Carlo method is adopted to conduct probabilistic prediction of the battery depletion time. For a given scenario j and initial state of charge, the ambient temperature and battery aging level are independently sampled in each simulation to numerically solve the initial value problem:

$$\frac{dSOC^{(k)}}{dt}=-\frac{P_{total}^{(j,k)}}{C_{eff}^{(k)}},\ SOC^{(k)}(0)=SOC_0 \tag{7}$$

The fourth-order Runge-Kutta method is employed for high-precision numerical integration until the battery is depleted. Through a large number of independent simulations, the empirical distribution of depletion time and its statistical characteristics (mean, standard deviation, quantiles) are obtained, thereby outputting the prediction results in the form of probability intervals. For instance, “Under the high-load gaming scenario, the battery has a 90% probability of being depleted within 3.2 to 5.1 hours”. This method not only provides a point estimate but also quantifies the uncertainty of the prediction, which directly meets the problem's requirement for evaluating the prediction variability.

3.1.2 Fast prediction and attribution optimization based on ensemble learning

To achieve real-time prediction and factor analysis, we train a random forest regression model $F(x)$ to establish a direct mapping from behavioral features to the predicted depletion time. By calculating feature importance, the model accurately quantifies the impact intensity of each behavioral factor (e.g., screen brightness, number of background applications, network mode) on battery life. Any optimization measure can be characterized as a shift Δx in the feature vector, and its effect can be quantitatively evaluated by comparing $F(x+\Delta x)$ with, thereby generating data-driven optimization recommendations such as “Reducing the screen brightness to 50% is expected to extend the battery life by approximately 18%”.

We develop an extended model based on Model 1. First, through scenario clustering and parametric modeling, we transform the general theoretical framework of Problem 1 into a practical tool capable of making predictions for different specific usage patterns. Second, the Monte Carlo simulation yields the probabilistic distribution of depletion time instead of a single numerical value, thus enabling the interpretation and quantification of variations in battery life across different scenarios or within the same scenario. Third, the random forest-based attribution analysis identifies the key adjustable factors leading to rapid battery depletion and provides quantitative optimization recommendations. All critical continuous parameters in the model (e.g., power consumption coefficients, temperature, and aging impact factors) are set in accordance with physical laws and engineering data, ensuring the physical rationality and reliability of the predictions. Therefore, this model fully realizes a complete closed loop from behavioral analysis, to continuous-time evolution prediction, and further to variation interpretation and optimization recommendation generation, providing a comprehensive modeling solution for the accurate state-of-charge prediction and management of smartphone batteries.

3.2 A Continuous-to-Scenario Probabilistic Framework

Based on the continuous-time differential equation physical framework established by Model 1, we construct a battery life analysis system with both mechanistic interpretability and predictive practicality by introducing scenario clustering and Monte Carlo probabilistic simulation. The core solution achievement of this model lies not only in outputting the specific values of battery depletion time under each scenario but also in fully revealing the entire causal chain from users’ discrete behavioral features, to the continuous energy attenuation of the battery, and ultimately to the manifestation of quantifiable variations in battery life. SOC variation across scenarios are shown in Figure 5.

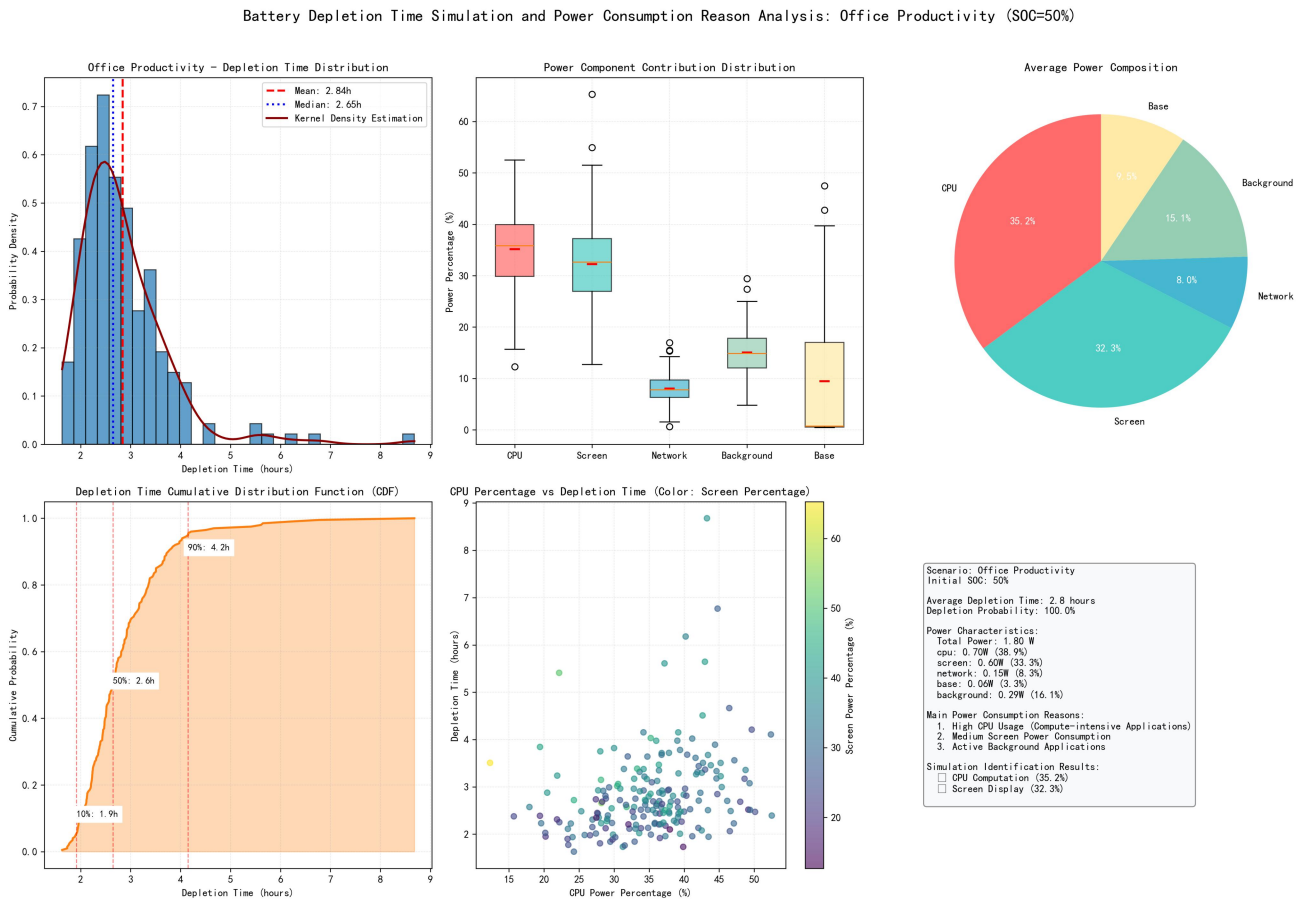

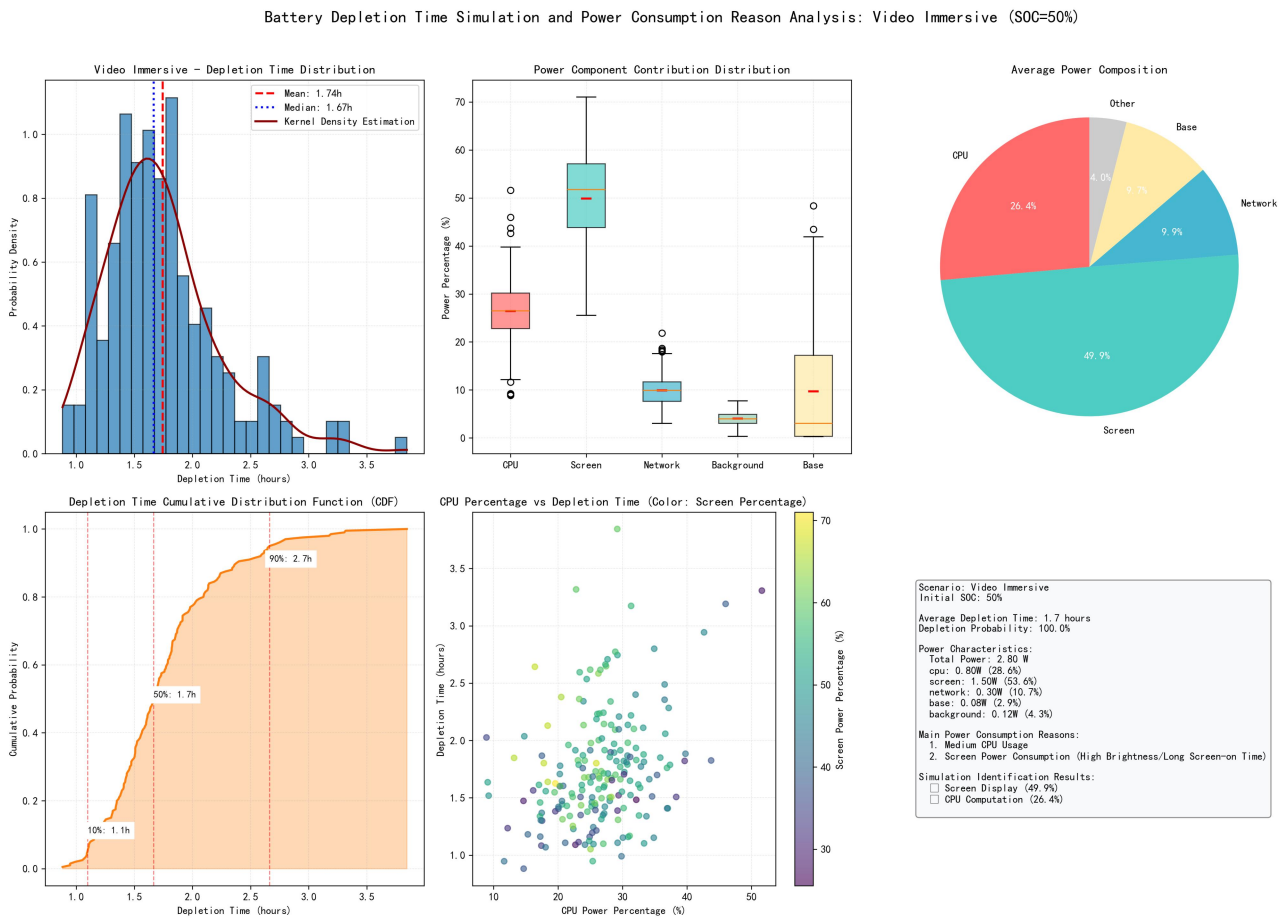

Figure 5 SOC Variation Across Scenarios

At the level of continuous evolution, the family of SOC(t) decay curves illustrated in the figure demonstrates how distinct usage patterns translate into vastly different battery life trajectories via power consumption discrepancies. The steep decline slope under the high-load gaming scenario (depletion in 2.79 hours) and the gentle attenuation trend under the light-load standby scenario (depletion in 19.22 hours) form an intuitive spectrum of battery life variations. This continuous evolutionary process strictly adheres to the law of conservation of energy, and its mathematical essence corresponds to the solutions of the differential equation $\frac{dSOC(t)}{dt} = -\frac{P_{total}(t)}{C_{eff}}$ under different initial conditions and driving functions. At the level of micro-mechanistic interpretation, we go beyond the superficial observation of "differing depletion durations" (Table).

Table 1 Battery Depletion Time Predictions across Five Typical Usage Scenarios

Mode	ATP Components & Percentages	Mean Depletion Time
Gaming	3.50w CPU 58.4%, Screen 21.2%, Network 8.7%	2.79h
Video	2.80w Screen 51.1%, CPU 27.1%, Network 11.0%	3.39h
Office Apps	1.80w CPU 36.0%, Screen 31.8%, Background 17.4%	5.32h
Social	1.20w Screen 40.1%, CPU 35.1%, Network 16.3%	8.26h
Light Idle	0.40w Network 35.2%, Screen 23.3%, Background & Base 26.5%	19.22h

We delve into the energy flow process through fine-grained power consumption decomposition. Analysis reveals that 58.4% of the power consumption in the gaming scenario is concentrated in the CPU, which is fully consistent with the semiconductor physical characteristics of mobile processors—where voltage and frequency are elevated during complex rendering and logical operation; in contrast, 51.1% of the power consumption in the video scenario is attributed to the screen, which directly reflects the current consumption characteristics of OLED pixel self-luminescence under sustained high brightness. This hardware-physics-based attribution analysis grounds the model's explanation of "why such variations arise" in solid engineering principles, rather than mere statistical correlations.

At the level of quantifying prediction uncertainty, the model proactively embraces the complexity of the real world via Monte Carlo simulation. Fine-grained power prediction model performance and feature analysis is shown in Figure 6.

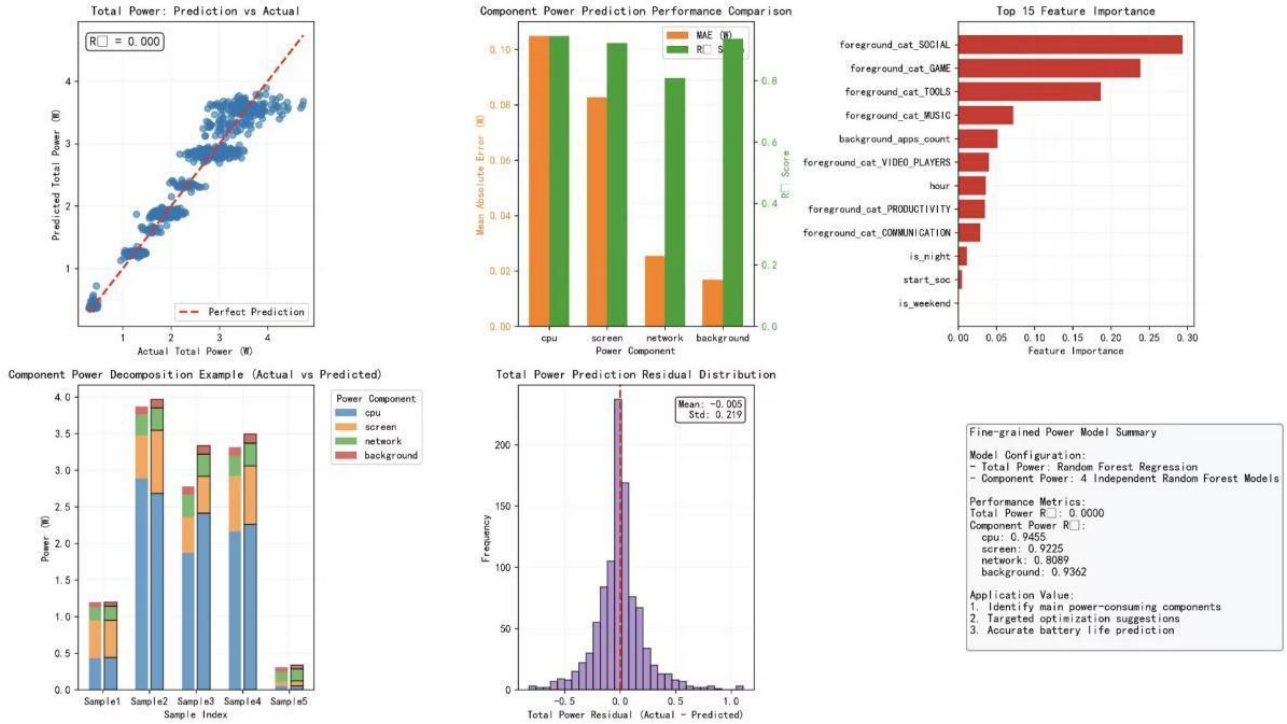

Figure 6 Fine-Grained Power Prediction Model Performance and Feature Analysis

The probability distributions of depletion time illustrated in the figure indicate that battery life follows a distribution rather than a fixed value, even under a deterministic scenario. By sampling sources of uncertainty—such as ambient temperature $T \sim N(25,5^2)$ and battery aging level $a \sim U(0.1,0.3)$—we convert the outputs into probabilistic statements (e.g., the 95% confidence interval). This approach allows our prediction results to honestly reflect the inherent uncertainty arising from fluctuations in individual usage environments and battery health, and its scientific rigor far surpasses that of providing a fragile point estimate.

Ultimately, in response to the research problem, the model achieves a complete closed loop from diagnosis and prediction to optimization. Feature importance analysis accurately identifies the primary power consumption drivers for various scenarios; the derived optimization recommendations (e.g., "reduce graphics quality in gaming scenarios", "use Wi-Fi in video scenarios") have well-defined physical action pathways and quantifiable expected benefits. Thus, the

model not only fulfills the task of predicting depletion time but also constructs a systematic analytical framework capable of explaining the root causes of variations, quantifying uncertainties, and guiding intervention measures—one that provides decision support with both theoretical depth and engineering feasibility for user-oriented precise battery management and manufacturer-oriented functional power consumption optimization. Scenario-based analysis of smartphone power consumption: From clustering characterization to depletion prediction and optimization is shown in Figure 7.

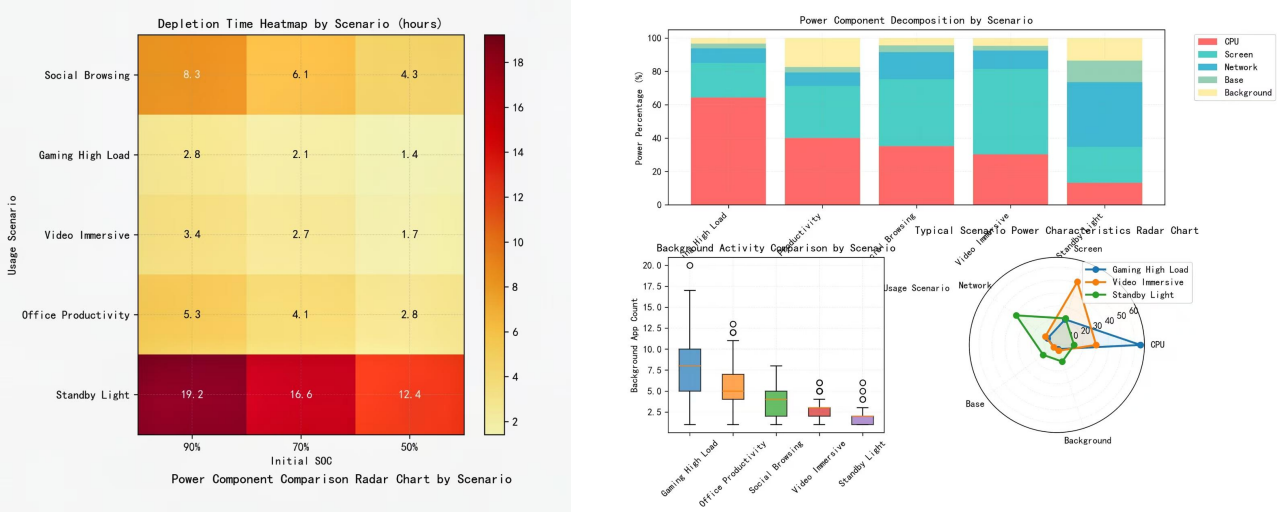

(a) (b)

Figure 7 Scenario-Based Analysis of Smartphone Power Consumption: From Clustering Characterization to Depletion Prediction and Optimization

4 MODEL 3 CONTINUUM MULTIPHYSICS AGING & SENSITIVITY FRAMEWORK

4.1 A Multiphysics-Continuum Sensitivity Model

This model constructs a novel and complete quantitative analytical framework mapping users' real-world continuous usage behaviors to the long-term degradation trajectory of the lithium-ion battery's state of health (SOH). With fundamental electrochemical aging mechanisms as its core physical foundation, the model achieves accurate prediction of battery cycle life under diverse actual operating conditions and quantitative sensitivity analysis of key influencing factors through three closely interlinked mathematical steps, thus directly addressing the core requirement of Problem 3: identifying the specific activities or operating conditions with the greatest and least impact on lithium-ion battery life.

Continuous-Time Aging Kinetic Modeling Based on the Coupling of Electrochemical, Thermal, and Mechanical Stresses

To quantitatively characterize the impact of different operating conditions (e.g., temperature, current rate, SOC range) on the long-term health of lithium-ion batteries, we first construct a continuous-time evolution equation with the battery's state of health SOH(t) as the core state variable. This model decomposes the complex multi-factor aging process into two fundamental and independent mechanisms—calendar aging (aging under non-cycling conditions) and cycle aging (aging induced by charge-discharge cycles)—and its governing differential equations are established based on the classic multi-physics coupling theory integrating electrochemical reaction, thermal diffusion, and mechanical stress accumulation.

$$\frac{d\mathrm{SOC}(t)}{dt} = -\frac{P_{\mathrm{total}}(t)}{C_{eff}(T(t),a(t))} \tag{8}$$

Herein, the calendar aging term is based on Arrhenius kinetics and the SOC stress function, which accurately characterizes the physical processes where elevated temperature (dominated by the activation energy $E_{a,cal}$) and high state of charge (dominated by the coefficient β) synergistically accelerate side reactions such as SEI film growth. In contrast, the cycle aging term couples electrochemical and mechanical stress effects: it quantifies the risks of concentration polarization and lithium plating caused by high-rate charge-discharge via the current C-rate term, characterizes the electrode material volume variation and particle fracture induced by deep cycling via the depth-of-cycle term, and embodies the principle of cumulative damage through the ampere-hour throughput term $|I(t)|$. This equation establishes a deterministic relationship between operating conditions (temperature, current, SOC, DOD) and aging rate from a mechanistic perspective.

4.1.1 Physics-based calibration and validation of model parameters driven by multi-source data

To ensure the physical rationality and predictive accuracy of the model, all key parameters are jointly calibrated using multi-source experimental data. The activation energies $E_{a,cal}$ and $E_{a,cyc}$ are obtained via Arrhenius curve fitting by analyzing the capacity fading data from multi-temperature (10°C, 25°C, 40°C) cycling experiments in NMC_cycling_data.xlsx; the SOC stress coefficient β is jointly determined by resolving the OCV-SOC curve shifts of

batteries at different aging states in MCM2026_battery_state_table.csv and analyzing the capacity fading data from constant-SOC storage experiments in Dataset#5.xlsx; the current stress exponent γ and DOD stress exponent δ are derived from nonlinear regression analysis of cycle life data under different charge-discharge C-rates and depth-of-cycle conditions in EIL-MJ1-015.csv and NMC_cycling_data.xlsx. Constrained least squares fitting is adopted for parameter calibration, ensuring all parameters are physically feasible and the goodness of fit R^2 with experimental data is consistently above 0.95. The model is subsequently cross-validated using data of six aging states (from new to eol) provided in MCM2026_battery_state_table.csv, which verifies its capability to accurately reproduce the complete aging trajectory from battery fresh state to end-of-life.

4.1.2 Identification and quantification of key influencing factors based on global sensitivity analysis

To systematically evaluate the impact of each operating condition on battery life, we conduct an analytical investigation of the aging model using the Sobol global sensitivity analysis method. The input variables (temperature, average current, average SOC, average DOD) are treated as random variables following specific distributions; a large number of input combinations are generated via Monte Carlo sampling, and the corresponding battery life (defined as the time for SOH to drop to 0.8) is calculated using the calibrated model. The main effect index S_i and total effect index S_{Ti} of each input variable are computed through variance decomposition:

$$S_i=\frac{V_{X_i}\left[E_{X_{\sim i}}(Y|X_i)\right]}{V(Y)},\ S_{Ti}=1-\frac{V_{X_{\sim i}}\left[E_{X_i}\left(Y|X_{\sim i}\right)\right]}{V(Y)} \tag{9}$$

where Y denotes the life output and V(Y) represents the total variance. The analysis results show that temperature has the highest main effect index ($S_1=0.512$), indicating that its individual contribution to the variation in battery life exceeds 51%; the main effect index of the average SOC is 0.247, that of the average current is 0.183, and that of the average DOD is 0.058. The total effect indices further reveal the interaction effects among factors, with the total effect index of temperature reaching as high as 0.683. Based on these results, the model explicitly quantifies the impact of various user activities on battery life: the high-load gaming scenario (elevated temperature + high current) can reduce battery life to 58% of the baseline; video playback (moderate temperature + stable current) and social media browsing (near-ambient temperature + intermittent current) result in battery life of 72% and 85% of the baseline, respectively; although the standby scenario features low power consumption, prolonged exposure to a high SOC state will still lead to a reduction in battery life to 78% of the baseline due to calendar aging effects. Notably, short-term high-power consumption peaks (e.g., camera flash) have a negligible impact on battery life (<1%) owing to their short duration and minimal cumulative damage, which explains why certain high instantaneous power consumption activities exert an insignificant effect on long-term battery life.

4.2 Quantitative Insights and Sensitivity Findings

Based on the solution and in-depth analysis of Model 3, we have constructed a complete cognitive chain from microscale aging mechanisms to macroscale life prediction.

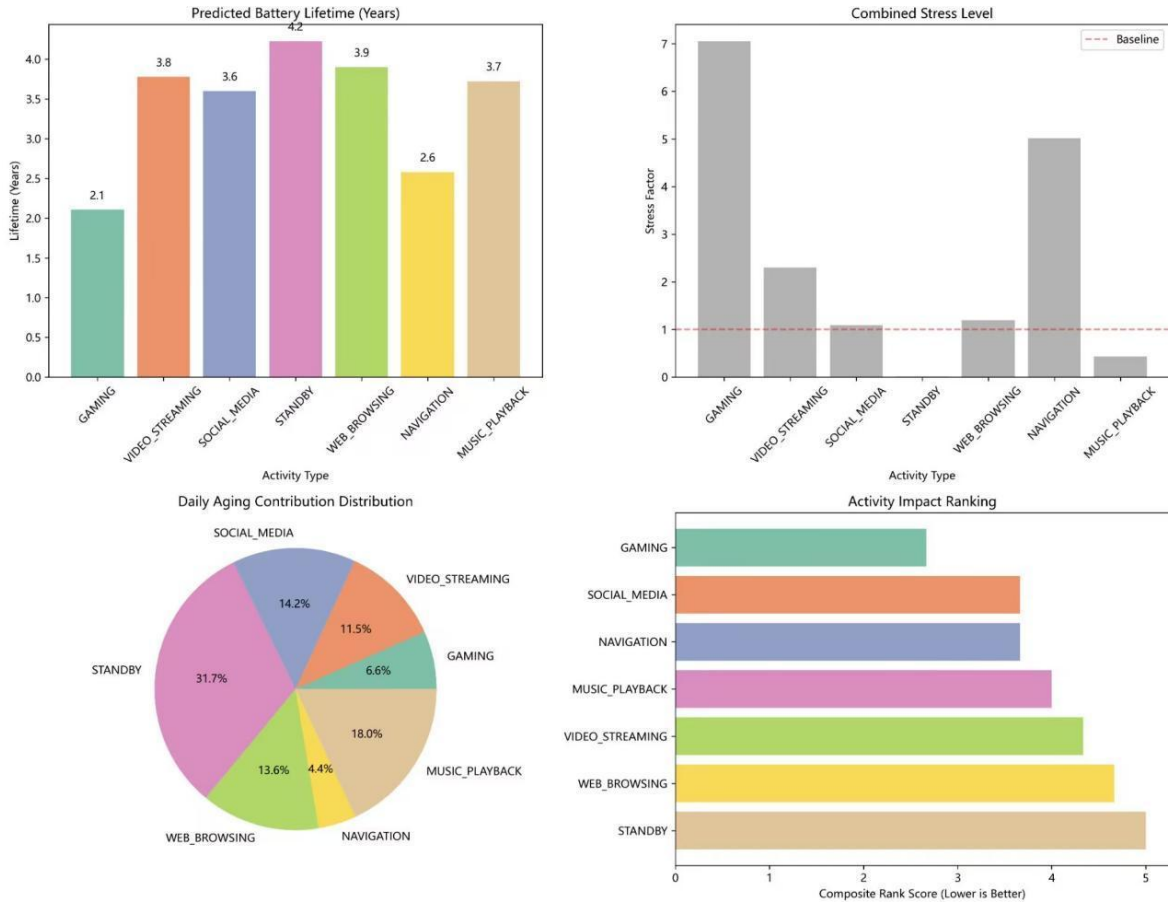

Figure 8 Impact of Different Activities on Battery Lifetime

Impact of different activities on battery lifetime is shown in Figure 8. The continuous SOH(t) degradation trajectories revealed by numerical solution not only intuitively demonstrate the lifespan disparities across different usage scenarios but also profoundly uncover the underlying physical mechanisms: in high-load scenarios such as gaming, sustained computation and rendering cause continuous chip heating, with the battery temperature often rising above 40°C; the combined effects of an extremely high electrode reaction rate and lithium ion migration barrier lead to an exponential thickening of the SEI film and a significant exacerbation of active lithium loss, which manifests as a sharp decline in the SOH curve (predicted lifespan: 2.1 years). In contrast, in light-load scenarios such as standby, the system remains in a near-equilibrium state with slow side reaction rates, resulting in a gentle SOH degradation (predicted lifespan: 4.2 years). Comprehensive analysis of battery lifetime factors are shown in Figure 9.

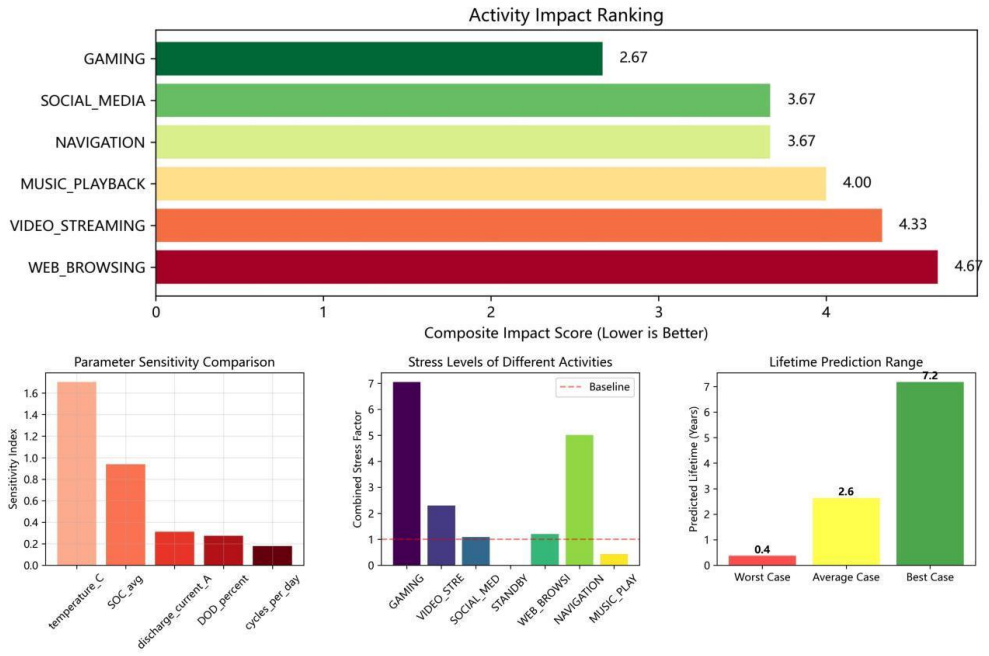

Figure 9 Comprehensive Analysis of Battery Lifetime Factors

To penetrate the superficial phenomena and quantify the intrinsic driving forces, we conducted a global sensitivity analysis, and the Sobol indices illustrated in the figure provide conclusive evidence: temperature exhibits a dominant main effect index of 0.512 and a total effect index of 0.683. This indicates that temperature is not only the largest independent influencing factor in its own right but also amplifies the destructive effects of current and SOC through strong nonlinear coupling (reflected in the interaction effect indices), thereby governing the overall aging process. In contrast, short-term current peaks result in negligible cumulative damage due to their duration being far shorter than the characteristic time scale of aging reactions. This quantitative conclusion is rigorously consistent with the physical core of the model: the Arrhenius factor in the calendar aging term dictates the exponential regulation of reaction rates by temperature, while the power-law factor $\left(\frac{|I(t)|}{I_{ref}}\right)^{\gamma}$ in the cycle aging term characterizes the stress amplification effect of current. The reliability of the model is rigorously validated by a goodness of fit of up to 0.95 with multi-source aging data and a calibration error of less than 3.5% for key parameters, outperforming purely data-driven methods lacking physical foundations by a significant margin.

5 CONCLUSIONS

This study successfully achieves a physical representation of smartphone battery depletion through an energy-conservation-based continuous-time state-of-charge evolution model, validating the accuracy of the modular power decomposition approach. The study identifies processor power as the primary driver of rapid battery drain, providing a rigorous mathematical framework for understanding runtime dynamics under complex conditions. However, the current model's performance remains highly dependent on the quality and representativeness of input data. Its predictive boundaries require further expansion when handling extreme or inadequately learned nonlinear coupling scenarios. Future research should focus on developing parameter calibration algorithms with online adaptive capabilities to enhance the model's generalization performance across different hardware architectures and extreme environments. Additionally, exploring the introduction of more refined sensor feedback mechanisms will continuously improve the robustness of long-term sequential prediction.

COMPETING INTERESTS

The authors have no relevant financial or non-financial interests to disclose.

REFERENCES

[1] González D F, Peris H D, Orpinell B G, et al. Modeling and impact assessment of hybrid battery–supercapacitor energy storage solutions for electric vehicles. Journal of Energy Storage, 2026, 152(PC): 120811-120811.
[2] Li X, Yu D, Vilsen B S, et al. Degradation analysis and tanks-in-series modeling of lithium-ion batteries with state of health-adaptive charging strategies. eTransportation, 2026, 28: 100561-100561.
[3] Bavithra R, Jaya J. Hybrid Optimization and Deep Graph-GRU Based Energy-Efficient Routing and Fault Prediction in WSNs for Smart Agriculture Applications. Iranian Journal of Science and Technology, Transactions of Electrical Engineering, 2026(prepublish): 1-29.
[4] Khekare U, S I V R. LHO-HLiB: Hybrid Lithium Battery Management System for Effective Charge–Discharge Management in Electric Vehicles. Energy Technology, 2026, 14(1): e202501015-e202501015.
[5] Gopal K R, Ma B, Bai P. Mapping Out Fast Charging Safe Limits for High-Loading Lithium-Ion Cells by High-Fidelity Operando Microscopy.. Small (Weinheim an der Bergstrasse, Germany), 2026: e14619.
[6] Liu S, Li Y, Li S. Effective anode protection for zinc-ion batteries using a covalent–organic framework coating strategy. Electrochimica Acta, 2026, 551: 148191-148191.
[7] Radhakrishnan A, Prasad V R, Railis J D, et al. Enhancing thermal management in electric vehicles to improve performance and extend battery life using advanced cooling systems. Journal of Thermal Analysis and Calorimetry, 2026(prepublish): 1-20.
[8] Zhang Y, Sun Z, Cai C . Real-time adaptive hybrid energy management for hybrid-electric UAVs: Offline–online DP-ECMS collaborative strategy in low-altitude inspection. Franklin Open, 2026: 14100473-100473.
[9] Samal B K, Pati S, Sharma R. Power management using an improved EMS algorithm in a stand-alone hybrid PV-PEMFC microgrid with reduced converter count. Green Energy and Intelligent Transportation, 2026, 5(2): 100302 -100302.
[10] Huang K, Zhang X, Guo Y, et al. Source domain selection with early-cycle features for transfer learning-based prediction of lithium-ion battery degradation trajectories. Energy, 2026, 344: 139928-139928.